Development of Large Linear Silicon Drift Detectors for the STAR Experiment at RHIC

R. Bellwied[4], R. Beuttenmueller[1], W. Chen[1], D. DiMassimo[1],
L. Dou[4], H. Dyke[2], A. French[4], J.R. Hall[4], G.W. Hoffmann[3],
T. Humanic[2], I. Kotov[2], H.W. Kraner[1], C.J. Liaw[1], D. Lynn[1],
S. Paganis[3], L. Ray[3], D. Read[3], V.L. Rykov[4], S.U. Pandey[2],
C. Pruneau[4], J. Schambach[3], J. Sedlmeir[1], G. Vilkelis[2], W.K. Wilson[4]
(STAR-SVT collaboration)

[1] Brookhaven National Laboratory
[2] Ohio State University
[3] University of Texas, Austin
[4] Wayne State University

Abstract

Large area linear Silicon Drift Detectors (SDD) are being developed for high energy and relativistic heavy ion collider experiments. SDDs have been proposed for the inner tracking detector in the STAR experiment at the BNL Relativistic Heavy Ion Collider to become operational in 1999. The Silicon Vertex Tracker (SVT) will consist of a three layer barrel structure composed of 216 individual detectors, each 6.3×6.3 cm^2. Prototypes, including one-way drift detectors (4.5×4.5 cm^2) and bi-directional drift detectors (6×6 cm^2) have been manufactured, and their properties have been studied. Design considerations, as well as test results, are presented in this article. Recent work has focused on minimizing the inactive guard structure area in order to optimize tracking efficiency. Particular attention is given to discussion of parameters that are sensitive to the reduced guard structure area, such as leakage current, maximum voltage and drift non-linearities.

1 Introduction

Successful linear drift detectors have been demonstrated in several publications [1,2,3,4,5] since the drift concept was developed by Gatti and Rehak [6]. Large area drift detectors are particularly well suited for big detector systems because of their cost efficiency. The STAR Collaboration (Solenoidal Tracker At RHIC) is designing a microvertex detector, the Silicon Vertex Tracker (SVT), which uses Silicon Drift Detectors (SDD) to measure charged particle hit positions near the beam vertex.

Careful measurement of the drift time in one dimension permits a spatial determination of the hit position to within 20 μm over a drift distance of as much as 4 cm. SDDs measure two dimensional position information unambiguously, using about one order of magnitude fewer channels than conventional strip detectors.

A disadvantage of the SDD, compared to strip and pixel detectors, is its slow collection time which limits the readout rate. By biasing the detector to 2000 V a maximum inverse drift velocity of about 1.5 μs/cm can be achieved. However, in STAR the maximum data collection rate is not limited by the SDDs but rather its main detector, a time projection chamber (TPC) with a drift time of about 50 μs. Because of the excellent spatial resolution and small pixel occupancy in the SVT and, given the hit densities expected from Au+Au collisions at RHIC, Silicon Drift Detectors therefore provide the most cost efficient silicon technology for STAR and similar large area collider experiments.

In the following sections we discuss the design and present test results of the first two prototype stages of the STAR SDD.

2 SVT and SDD prototype design

The SVT will use 216 6.3 $\times$ 6.3 cm^2 SDDs in a three concentric barrel design, having radii of 7, 10.5, and 14.5 cm, respectively, to cover an angular range up to $\pm$ 45 degree in polar angle (Θ) and 2 π in azimuth. The three barrels consist of 8, 12, and 16 ladders, holding 4, 6, 7 wafers, respectively. The structural design is comparable to that of existing micro-vertex detectors used by CDF, ALEPH, and DELPHI.

A first prototype device, STAR1, was designed and developed using 75 mm diameter neutron transmutation doped (NTD) silicon exhibiting high and uniform resistivity ($\approx$8 KΩcm). The maximum STAR1 detector size is 4.5 $\times$ 4.5 cm^2, resulting in 179 anodes with a 250 μm spacing. The cathode pitch is 120 μm. The device is configured as a one-directional drift detector. Five (5) successful STAR1 devices were produced and tested [7]. The STAR1 design requires a significant inactive guard area (22% of the total area) to support the high biases (up to 2500 V) on the detector. This inactive area leads to large tracking inefficiencies, because the mechanical design of the SVT as well as radiation length constraints do not allow the overlap of detectors.

A second prototype series, started as STAR2, was produced with the emphasis given to achieving a full size detector for the experiment with a maximized active area. By using 100 mm diameter silicon, a square device of 6.3 $\times$ 6.3 cm^2 can be realized and with drift of 30 mm to collecting anodes at opposite edges from a central bias one can achieve a 95%

active area with a reasonable applied bias of up to 2000 V. Several designs of two-way drift configurations within this envelope have been recently produced at BNL. NTD 100 mm diameter float zone refined wafers have been obtained from Wacker for these prototypes as well as the later production devices for the experiment. They are 3 kΩcm, 1,1,1 material, 300 μm thick. The material has been qualified by fabricating several wafers with small diodes across diameters, which permits C(V) measurements indicating nominal uniform resistivity across the entire diameter to within 5%.

Two main issues have been addressed in the STAR2 prototype: (1) maximizing the active area on the wafer by reducing the guard area, and (2) minimizing the on-detector power dissipation by reducing several inherent device currents. The main consideration in reducing inactive area devoted to the guard structure was the understanding that the maximum applied bias at the center of the detector, 2000 V, will deplete $\approx$ 1.2 mm, which would be the distance from a central high bias contact outwards to the device edge which should be at ground potential. If the surface potentials were constrained to follow the bulk potentials by the means of a guard structure, this is the maximum distance required for a guard structure. One can add 1 mm for wafer cutting and handling and arrive at an inactive edge dimension of 2.2 mm.

The STAR1 guard structure was formed by p+ implantations; for STAR2, it was suggested that the guard structure could be created by field plates, metal over the field oxide, basically following the implanted structure pattern. This permits some mask level simplification as variations in field plate design can be made by changing only the final metalization mask. In the first STAR2 prototype run, four field plate designs were tried in a batch of nine wafers. The two principle designs were field plate versions of implanted guard designs which derived potentials from cathode strips to uniformly drop the surface potential with $\approx$ 20 equipotential plates. Two different pitches of field plates were tried. Fig.1 shows the central region of the version STAR 2.7 with the field plate structures extending 1.2 mm from the cathode strip ends towards the wafer edge. The pitch of the guard strips is 55 μm and they are connected to every tenth cathode strip which places about 68 V between each guard strip. Numbers to identify cathode positions are also shown. The metalization connects the numerically identical cathode on each side of the central high voltage bias which permits connection to an external voltage divider to be made only on one half of the detector; this is a necessary condition for mounting the final detector configuration. A band of implanted n+ contact to fix the edge potential at ground is shown just towards the edge outside of the numbers. Simulations have indicated that this distribution of surface potential results in nearly uniform equipotentials throughout the bulk, however several regions of high lateral fields persist in the bulk near the interface at the edges of the field plates, due to the accumulated interface positive charge. The STAR 2.7 prototype was made in a batch of 15 wafers of which 5 were suitable for reliable testing. This batch included both field plate and implanted guard structures; a clear decision on the best design awaits further tests.

Fig.1 also shows a pad contact on each side of the central bias contact which is a metalization covering an n+ implant used for charge injection by a negative external pulse. Injection lines are provided in between cathode strips at positions of 0.1, 1, and

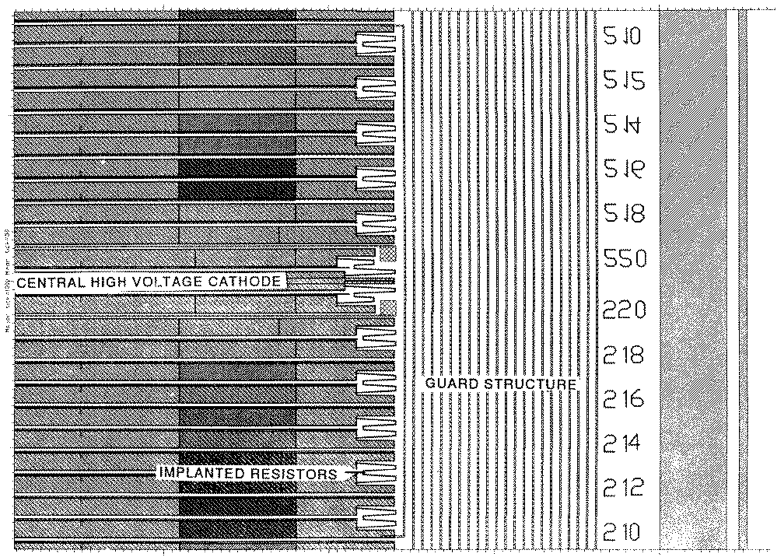

Figure 1: Central portion of STAR 2.7 showing field plate guard structure, resistor geometry, central injector line and edge treatment. The guard strips are placed on 55 μm pitch.

2 cm from the anode edge as well. Results indicate that the uniform implanted line works well. Fig.1 also shows the shape of the integrated resistors connecting the cathode strips at alternate ends of the cathode strip. A single p+ boron implant covering the cathodes themselves and the resistor structure of $1.15\times 10^{13}/\mathrm{cm}^2$ has proven to produce a sheet resistance of about 5 kΩ/sq with a particular annealing schedule. The resistor pattern shown in Fig.1, STAR 2.7, gives a 190:1 aspect ratio increasing the value to 1 MΩ and thereby reducing the standing current and power dissipated on the resistor chain. Measurements of groups of resistors verify these numbers; test resistors are included in test structures around the periphery of the fabricated wafer.

When the detectors are biased using only their own implanted resistor chains, the potential gradient is not linear along the detector as desired but develops a quadratic dependence on position; therefore a stiffer external voltage divider with contact to every fifth cathode strip is used as well. The effect is caused by the holes, thermally generated under the oxide and collected by the adjacent cathodes which thus contribute to the internal resistor divider current. This phenomenon may ultimately limit the highest value of resistance of the internal resistance chain. High resistance reduces the heat which must be removed from the detector in order to achieve a uniform temperature distribution across the drift region, and hence a uniform drift time, but the smaller current flowing in the resistor chain will be affected more easily by leakage currents.

3 Results

For detector testing, a calibrated laser diode is used which generates a charge deposition within a dimension of $\approx 5\mu$m, approximately equivalent to that due to minimum ionizing particles. The laser intensity can be varied to create local ionization over a wide range of charge deposition from $\sim (2-3)\cdot 10^4$ to about $7{\cdot}10^5$ electrons per pulse. These levels correspond to expected ionization levels for particles created in RHIC Au-Au collisions, which range from minimum ionizing (MIP) particles to slow protons with momenta down to $\sim$ 100 MeV/c ($\approx$ 30·MIP). A maximum bias of 2000 V over 30 mm drift leads to a maximum drift time is 4.5μs with a drift velocity of $6.7\mu m/ns$. By moving the laser spot across the SDD surface in both lateral and drift direction, the signal dependencies on the primary ionization position are studied.

With few exceptions, prototype drift detectors that have been tested with laser pulse injection have indicated linear drift time/position responses in agreement with the literature. Varying the drift field between 300 and 500 V/cm for both STAR1 and STAR 2 devices has yielded measured electron mobilities of 1333 cm^2/Vs ($\pm$5%), very close to the nominal room temperature value. To further test the drift homogeneity of a large drift device, the response of every tenth anode of a STAR 2 detector was measured and is shown in Fig.2. The general homogeneity is apparent and examination of the differential non-linearities associated with this measurement indicated a $\sigma \approx 2$ ns, or 10 μm (using 0.2 ns/μm).

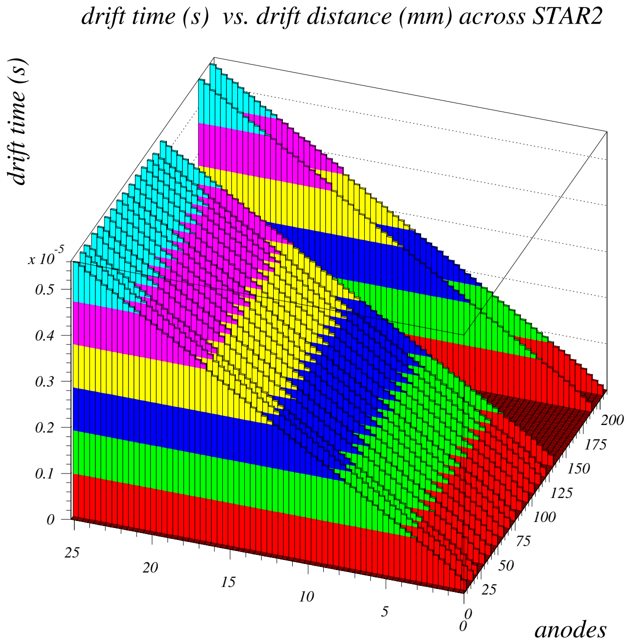

Figure 2: Drift-time versus drift distance for many anodes on a STAR 2 prototype biased with the external voltage divider, which is connected to every 5th cathode strip on the wafer.

Fig.3 shows the precision of the position measurement for repeated laser injection at a fixed drift length (20 mm) and a fixed bias (1500 V, 375 V/cm) on a STAR1 detector. Fig. 3a shows the observed precision in the drift direction, Fig. 3b shows the precision in the lateral or anode direction. The measured resolutions (σ) are 6μm in the anode direction and 24 μm in the drift direction. The measurement in drift direction is in agreement with the resolution measured for a radial drift detector [8]. The improved σ in the anode direction is due to the rather limited lateral spread of the charge cloud. Based on the chosen running conditions (maximum voltage, number of timebins) the charge cloud arriving at the anodes is more distributed in drift direction than in anode direction. The signal levels on each anode are therefore large enough to be less susceptible to excessive electronic system noise, caused by anode current or other electronic sources. The running conditions can be modified to yield a comparable position resolution in both directions (about 15 μm).

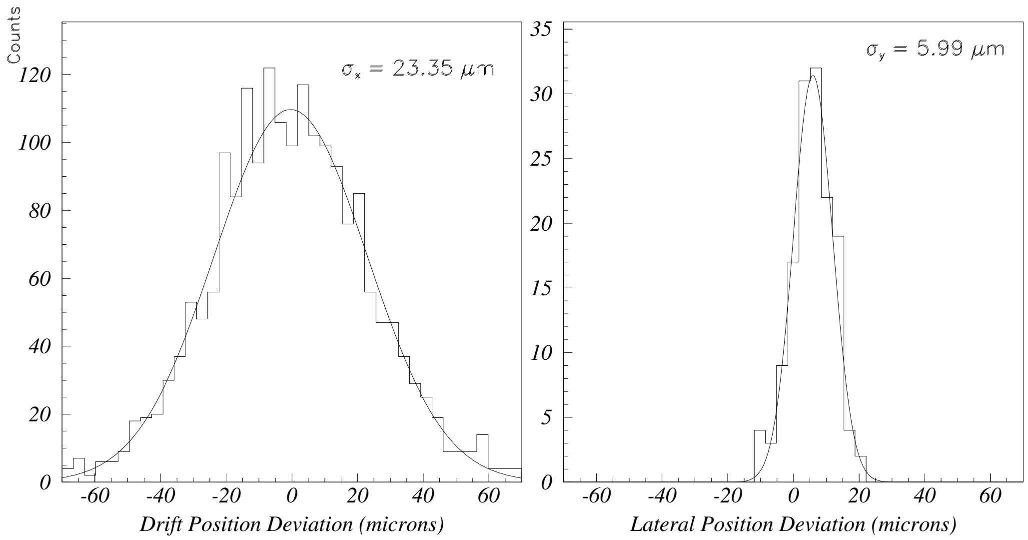

Figure 3: a.) Precision in the measured drift time after correction for temperature effects. b.) Precision in the measured lateral position

During the bench measurements of several STAR1 detectors the temperature of the detector was observed to rise by a few degrees as monitored by a thermistor on the device. A correlation between drift time and temperature was determined which confirmed the dependence $v_{drift} \propto T^{-\alpha}$, where α equals 2.4 [9]. Fig. 4 displays this correlation.

On-wafer temperature sources that could cause temperature gradients and drift non-uniformities include the on-wafer resistor chain and surface currents; these power sources must be minimized and should not exceed 100 mW.

On STAR1 the guard anode currents were generally on the order of 5 μA with almost all signal anode currents below 100 nA. The design changes on the STAR2 detectors have lead to increased anode currents up to several μA. Some fraction may be due to undesirable charge injection from the p-n junction breakdown between the n+ anode implant and the

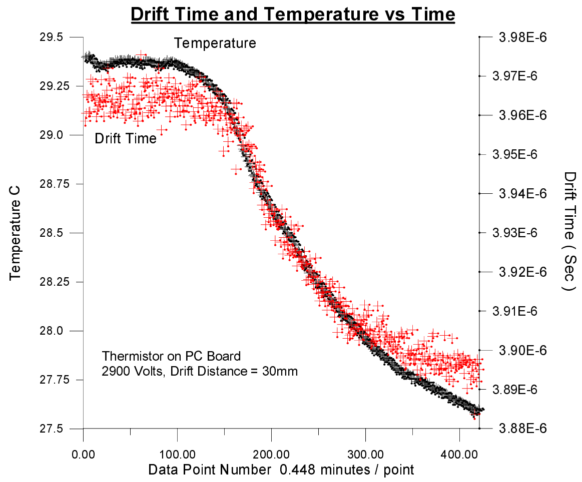

Figure 4: Drift-time and temperature correlation as function of time.

surrounding p+ implant. The guard anode currents have approached values up to 1 mA, which may be due to a true surface component and an injected component. The cause of the high currents in STAR2 has to be resolved for the final design in order to keep the dissipated on-wafer power below 100 mW. However, several STAR 2 detectors, based on the design as shown in Fig.1, have yielded low anode currents, generally $\leq$10 nA.

Additional tests were performed to determine the breakdown voltage for the different STAR2 field plate designs. With the design shown in Fig.1 biases up to 1800 V were generally achieved. The SVT requires a maximum voltage of 1400 V.

The anode region of a SDD has several separate surface electrodes to guide, under appropriate bias, the drifting charge cloud to the detector surface at the anode. The slightly lower resistivity of the 10 cm NTD material used in STAR 2 leads to voltage differences approaching 100 V between the anode (at ground) and the opposite side of the detector to provide the proper focus. Optimal focusing voltages vary slightly from detector to detector.

4 Summary

The present set of prototypes of large area, linear drift detectors for STAR have provided important results to further optimize the design of the final SDD. The detectors exhibited excellent position sensitivity and linearity. The response of the detectors is well understood from an analytical point of view.

The STAR experiment requires that the SDDs have a maximum active-to-guard area of 95%. Therefore special emphasis was given to a design that optimizes the ratio of active to guard area on the detector. In these mini-guard detectors no major problems have been found in the actual drift properties and the application of sufficient bias voltage. Guard anode currents are still somewhat higher than the final requirements, but a solution to this problem is expected for the next prototype design.

5 Acknowledgments

The efforts of Pavel Rehak, Charles Naudet, and Grazyna Odyniec in the design and testing of the STAR1 prototype are gratefully acknowledged. We appreciate very helpful discussions with Josef Kemmer and Gerhard Lutz.

This work was supported in part by the U. S. Department of Energy (under contract No. DE-AC02-76CH00016 and others), the National Science Foundation and the Robert A. Welch Foundation.

6 References

[1] J. Ellison et al., Nucl. Inst. and Meth. A260 (1987) 353
[2] A. Vacchi et al., Nucl. Inst. and Meth. A326 (1993) 267
[3] B. S. Avset et al., Nucl. Inst. and Meth. A310 (1991) 203
[4] W. Chen et al., IEEE Trans. Nucl. Sci., NS-39 (1992) 319
[5] M. Clemen et al., Nucl. Inst. Meth. A316 (1992) 283
[6] E. Gatti and P. Rehak, Nucl. Instr. and Meth. 225 (1984) 608
and Nucl. Instr. and Meth. A235 (1985) 224.
[7] S. U. Pandey et al. (SVT collaboration), Nucl. Inst. and Meth. A361 (1995) 457
[8] W. Chen et al., Nucl. Inst. and Meth. A326 (1993) 273
[9] S.M. Sze, *Physics of Semiconductor Devices (2nd ed.)*, Wiley, New York, 1979